

Microwave control of directed transport in asymmetric antidot structures

A.D. Chepelianskii^a

École Normale Supérieure, 45, rue d'Ulm, 75231 Paris Cedex 05, France

Received 7 May 2006

Published online 31 July 2006 – © EDP Sciences, Società Italiana di Fisica, Springer-Verlag 2006

Abstract. It is shown that a polarized microwave radiation creates directed transport in an asymmetric antidot superlattice in two dimensional electron gas. A numerical method is developed that allows to establish the dependence of this ratchet effect on several parameters relevant for real experimental studies. It is applied to the concrete case of a semidisk Galton board where the electron dynamics is chaotic in the absence of microwave driving. The obtained results show that strong currents can be reached at a relatively low microwave power. This effect opens new possibilities for microwave control of transport in asymmetric superlattices.

PACS. 05.45.Ac Low-dimensional chaos – 05.60.-k Transport processes – 72.40.+w Photoconduction and photovoltaic effects

1 Introduction

The appearance of a directed transport induced by radiation in asymmetric systems is known as the photogalvanic effect. By this effect the radiation creates charge transport in the bulk of the asymmetric structure in absence of any applied *dc*-voltage. The theoretical investigations of this phenomena have been started almost 30 years ago in references [1,2]. The interest to this subject has been renewed recently with the studies of ratchets that appear when a system is displaced from thermal equilibrium by a periodic variation of system parameters (for reviews see references [3,4]). These parameters can be treated as generalized forces. One of the surprising properties of ratchets is that a zero mean force can still produce a directed flow of particles. This phenomenon has a generic origin and appears in various physical systems including vortices in Josephson junction arrays [5–7], cold atoms [8], macroporous silicon membranes [9], microfluidic channels [10] and other systems.

Nowadays technology allows to prepare artificial antidot superlattices in semiconductor heterostructure with two dimensional electron gas (2DES). The conduction properties of these samples has been tested in experiments [11,12] which showed an important contribution of periodic orbits. The structure of these superlattices is similar to a periodic lattice of rigid disks placed on a plane. Such structures are known as Galton boards [13] or Lorentz gas. According to the mathematical results of Sinai the dynamics on such a lattice is completely

chaotic [14]. The theoretical studies [15] performed to understand these experiments showed that the chaotic classical dynamics and periodic orbits significantly affect the conduction properties in such superlattices.

The effect of a microwave radiation on the conduction properties of an antidot superlattices has been addressed in experiments [16]. However in these structures due to the symmetry of the superlattice the ratchet effect was forbidden. Asymmetric mesoscopic structures under external periodic driving have been studied experimentally in [17]. However zero mean force ratchet was absent due to low frequency of driving which was essentially adiabatic [18].

The recent theoretical studies of dissipative transport in asymmetric superlattices showed that microwave radiation induces directed transport in such systems (zero mean force ratchet) [19,20]. These works were mainly performed for a semidisk Galton board which is obtained from the usual Galton board of rigid disks by replacing each disk with semidisk oriented in one fixed direction (see Fig. 1). In reference [19] the model of a friction force $\mathbf{f}_f = -m\gamma\mathbf{v}$ with constant friction coefficient γ has been used for a particle of mass m moving with velocity \mathbf{v} . In reference [20] the case of particles in a Maxwell thermostat at temperature T was considered. It was shown that the thermostat creates an effective friction coefficient γ which depends on the microwave field strength and the temperature of the thermostat. However the most interesting case is the Fermi-Dirac thermostat since it describes the experimental conditions of antidot superlattices with 2DES [21]. Until now no numerical studies were performed in this regime. Only theoretical estimates have been proposed in

^a e-mail: alexei.chepelianskii@ens.fr

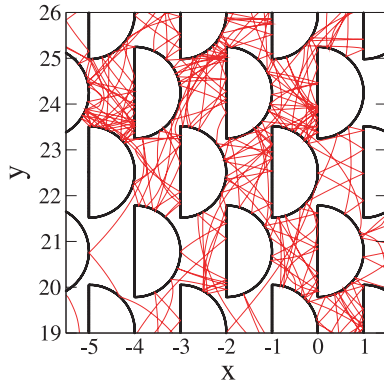


Fig. 1. (Color online) Example of the semidisk Galton board with one chaotic trajectory in the region $-5.5 \leq x \leq 1.5$ and $19 \leq y \leq 26$. Semidisk scatterers, separated by a distance $R = 2$, are shown in black. The trajectory is displayed in red/gray. The strength of microwave radiation and its frequency are $f = 5$, $\omega = 1$, polarization angle $\theta = 0$ and temperature $T = 0.1E_F$. Here and in other figures $E_F = 10$ and disk radius $r_d = 1$. The Metropolis algorithm parameters are $\Delta E/E_F = 0.075$, $\Delta t = 0.005$.

reference [20]. Their validity was never checked and remains questionable.

In this work I develop a numerical method which allows to study the directed transport induced by polarized microwave radiation $\mathbf{f} = f(\cos \theta, \sin \theta) \cos(\omega t)$ in 2DES at various values of the Fermi energy E_F and temperature T (here ω is the radiation frequency and θ is the polarization angle with respect to the x axis in Fig. 1). On the basis of this method I performed extensive numerical studies which allowed to establish the dependence of ratchet flow velocity v_f on various system parameters including T and E_F . Contrary to the estimates proposed in reference [20] the dependence on T is weak when $T \ll E_F$. The obtained results allow to predict typical values of currents in asymmetric antidot superlattices.

The paper is organized as follows, in Section 2 the description of the model and of the numerical method is presented, the results are described in Section 3, and conclusion is given in the last section.

2 Model description

The geometry of the model is represented by a Galton board of semidisks which form a two-dimensional hexagonal lattice as shown in Figure 1. The radius of the semidisk is r_d and the distance between the disk centers is R . A particle with mass m moves under the action of the electric force \mathbf{f} of a polarized microwave radiation. The collisions with the semidisks are elastic. In the numerical simulations I use dimensionless units with $m = r_d = 1$ and the Fermi energy $E_F = 10$ (thus the Fermi velocity $V_F = \sqrt{20}$). In order to convert the numerical results obtained with this units, one should determine the dimensionless ratios: for example in Figure 1 the frequency $\omega = 1$

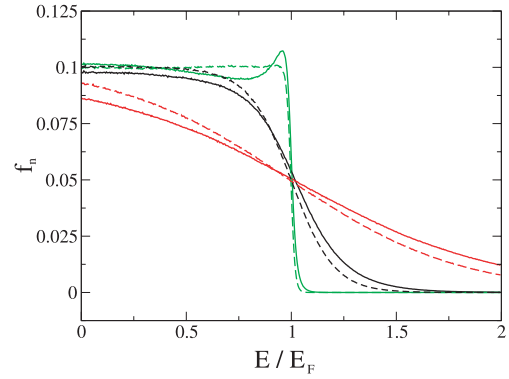


Fig. 2. (Color online) Energy distribution functions $f_n(E)$ obtained numerically for different field amplitude values f and different temperatures T . For the green, black and red curves the temperatures are $T/E_F = 0.01$, 0.1 , and 0.4 respectively (at $E/E_F = 1.1$ the order of curves is from bottom to up). The applied force f is zero for the dashed curves and $f = 5$ for the full curves ($\omega = 1$, $\theta = 0$, $R = 2$). At $f = 0$ the dashed curves coincide with the Fermi-Dirac distribution $f_F(E)$ at corresponding temperature T . The Metropolis algorithm parameters are the same as in Figure 1.

and field strength $f = 5$ corresponds to dimensionless values $\tilde{\omega} = \omega r_d/V_F = 1/\sqrt{20}$, and $\tilde{f} = f r_d/E_F = 1/4$.

It is assumed that particles are non interacting but that the contact with a thermostat creates the Fermi-Dirac distribution $f_F(E) = 1/(E_F[\exp((E - E_F)/T) + 1])$ at temperature T and Fermi energy E_F , where E is a particle kinetic energy. Here the energy distribution for one particle $f_F(E)$ is normalized by the condition $\int f_F(E)dE = 1$. This single particle distribution gives also the result for many particles by simple rescaling by the number of particles as it is usually done for 2DES (see [21], p. 193). Such a situation corresponds to experiments with 2DES in antidot lattices similar to those of references [11, 12]. To keep particles in a thermal equilibrium with the Maxwell distribution it is possible to use various methods including the Nosé-Hoover thermostat used in reference [20]. However for the Fermi-Dirac thermal distribution this method is not appropriate and a new approach should be developed. Indeed the Nosé-Hoover equations are constructed in such a way that they give the Maxwell distribution in particle velocities [22, 20]. They should be significantly modified to generate the Fermi-Dirac distribution and until now this problem has not been addressed yet. The first attempt by the authors of reference [20] did not succeed in achieving a good convergence to the Fermi-Dirac distribution [23].

My approach is inspired by the successful Monte Carlo method adapted to simulate numerically the transport properties in semiconductor devices [24]. To obtain a stable Fermi-Dirac distribution of particles on the semidisk Galton board (see Fig. 1) the following procedure has been applied: (i) the equations of motion were integrated exactly on the time interval Δt using the analytical solution; (ii) after that the particle energy is changed from its value E to another value in the interval $(E - \Delta E, E + \Delta E)$ without changing the direction of the particle momentum.

The choice of this value is governed by the Metropolis algorithm [25] which imposes the convergence to the Fermi-Dirac distribution f_F . Namely, a random value E' is chosen in $(E - \Delta E, E + \Delta E)$, with probability $\min(f_F(E')/f_F(E), 1)$ the algorithm sets $E = E'$, otherwise E remains unchanged. Afterward the algorithm returns to step (i). The times when collisions with semidisks occur are found with the precise Newton algorithm as in reference [19]. The step ΔE can be considered as a thermalization step which determines the rate of convergence to the equilibrium distribution f_F .

The Metropolis algorithm described above ensures the convergence to the equilibrium distribution f_F in the absence of microwave radiation. The examples of steady state distributions at different temperatures T are shown in Figure 2. The proximity of the numerically obtained distribution $f_n(E)$ to the theoretical steady state $f_F(E)$ can be characterized by the dimensionless mean square deviation $\sigma = E_F \int (f_n(E) - f_F(E))^2 dE$. This quantity remained small in all numerical simulations at $f = 0$ showing a good convergence to the Fermi-Dirac distribution (e.g for the cases of Figure 2: $\sigma = 1.8 \times 10^{-5}, 2.3 \times 10^{-5}$ and 8.3×10^{-5} for $T/E_F = 0.4, 0.1, 0.01$ respectively). In the absence of microwave field driving the Metropolis algorithm reproduces the Fermi-Dirac distribution with high accuracy therefore the heat capacity of the simulated 2DES is in agreement with the usual relations for the Fermi gas and is linear in temperature [26,27]. Special numerical checks have shown that a weak static electric field creates a stationary current and that the low frequency conductivity σ_0 obtained numerically is in agreement with the Drude formula $\sigma_0 = n_e e^2 \tau / m$ which is valid for a degenerate Fermi gas [26,27]. For quantum systems the exact expression of the conductivity is given by the Kubo formula, which leads to the classical Drude result in the case of a Fermi gas at high quantum numbers [28]. At last, although the Metropolis algorithm has been introduced in a formal way in order to guarantee the convergence to the Fermi-Dirac statistics, it can be considered as an approximation of the electron relaxation at low temperatures. Indeed in real metals the energy distribution function is controlled by electron-electron and electron-phonon scattering, which conserve the direction of motion but loose energy. The later property is also present in the proposed method.

However, the introduction of the microwave radiation modifies the distribution f_n which depends on f and other system parameters. This is clearly seen in the typical cases presented in Figure 2. For relatively high temperatures the distribution f_n remains a smooth monotonic function of energy whereas at low T the microwave field creates a characteristic peak near the Fermi energy E_F . As a result the developed numerical method allows to study the transport created by microwave radiation in an asymmetric semidisk Galton board in the stationary regime. To be close to realistic experimental situations additional random scattering has been introduced to take into account the effect of impurities. Namely after time τ_i the direction of particle momentum is changed randomly (angle changes

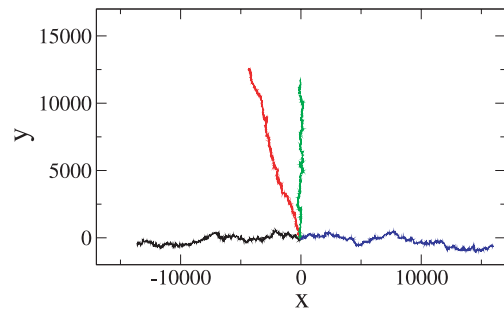


Fig. 3. (Color online) Directed transport for one trajectory at various polarizations of radiation $\theta = 0, \pi/5, \pi/4, \pi/2$ (from left to right clockwise), other parameters are set as in Figure 1.

in the interval $[0, 2\pi]$). In the majority of cases studied the value τ_i was kept sufficiently large ($\tau_i V_F / r_d > 1000$) and did not influence the stationary transport properties (the dependence on τ_i will be discussed in the next section). Here $V_F = \sqrt{2E_F}$ is the Fermi velocity.

This stationary regime, which sets in presence of radiation, clearly shows the photogalvanic (ratchet) effect with directed transport born from chaos as it is shown in Figure 3 for different polarization angles θ . I would like to stress that this effect originates from the bulk of the sample; it is known that radiation can lead to the appearance of electron-hole pairs, which may diffuse to different contacts because of the electric field in the depletion region of the junction, however in this case the effect is due to the contacts and not to the bulk of the sample. For $\theta = 0$ the transport is directed to the left (negative direction on the x axis), while for $\theta = \pi/2$ the transport is oriented to the right. The polarization dependence is similar to that obtained in previous works [19,20] and is well described by the relation $\psi \approx \pi - 2\theta$ where ψ is the angle between the transport direction and the x axis. In this way the average velocity of transport can be written as $\mathbf{v}_f = v_f (\cos \psi, \sin \psi)$. It is calculated by following a single trajectory for a long typical time $tV_F / r_d \sim 10^7$. It was also checked that the averaging over an ensemble of few tens of different trajectories gives statistically the same result.

Special checks have been made to ensure that the ratchet velocity v_f does not depend on the Metropolis algorithm parameters. An example of such checks is shown in Figure 4 where the thermalization step ΔE was changed by one order of magnitude. In spite of this variation the value of v_f remains stable. It was also checked that the resulting ratchet velocity is not sensitive to variation of Δt , e.g a variation of Δt by more than one order of magnitude gave no variation of v_f within a 5% accuracy. Physically it is possible to say that the relaxation time to the equilibrium τ_{rel} is approximately given by the relation $\tau_{rel} \sim \Delta t E_F^2 / \Delta E^2$. Thus, the numerical checks above can be physically interpreted as the independence of the ratchet velocity on the variation of the energy relaxation timescale τ_{rel} which varied by two orders of magnitude. A similar effect has been seen with the Nosè-Hoover thermostat for the Maxwell equilibrium distribution [20]. This

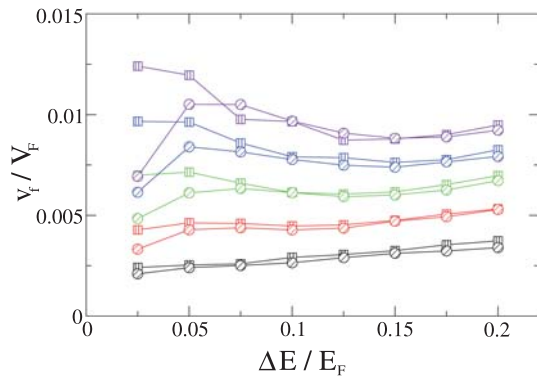


Fig. 4. (Color online) The ratio of flow velocity v_f to the Fermi velocity V_F as a function of the thermalization step ΔE for a fixed $\Delta t = 0.005$. The different curves correspond to values of f : $f = 7.0, 6.0, 5.0, 4.0, 3.0$ with respective colors: violet, blue, green, red, black (from top to bottom at $\Delta E/E_F = 0.2$). The symbols mark the temperature $T/E_F = 0.01$ (squares) and $T/E_F = 0.1$ (circles). Other parameters are as in Figure 1.

result is also in a qualitative argument with the theoretical arguments given in references [1,2] according to which τ_{rel} does not directly affect v_f . In my further simulations the Metropolis algorithm parameters are set to typical values $\Delta E/E_F = 0.075$, $\Delta t = 0.005$. The data shown in Figure 4 clearly demonstrate that v_f grows with the radiation strength f . At the same time v_f is not very sensitive to the variation of temperature T . Detailed studies of parameter dependence of v_f are presented in the next section.

The results presented above show that in the absence of electron-electron interactions, the developed algorithm allows to simulate the electron dynamics at thermal equilibrium with the Fermi-Dirac distribution. The microwave driving is assumed to be relatively weak so that it gives only small deviations from the unperturbed distribution, this fact is clearly illustrated in Figure 2. In this regime the perturbed distribution of particles is determined by the unperturbed distribution $f_F(E)$ and the microwave field, the effect of the latter is exactly taken into account by the Hamiltonian equations of motion. Therefore the developed algorithm should correctly describe the non equilibrium steady state distribution that emerges under microwave driving. This is indirectly confirmed by the fact that the directed transport is not sensitive to the thermalization step of the Metropolis algorithm (see Fig. 4). In a sense the Metropolis steps combined with the Hamiltonian equations of motion give the solution of the kinetic Boltzmann equation in the presence of microwave driving.

The above arguments should be also valid for another unperturbed thermal distribution, e.g the Maxwell distribution $f_M(E) = \exp(-E/T)/T$. This case was analyzed in reference [20] on the basis of Nosé-Hoover equations. In fact the Metropolis algorithm had been invented to treat the Maxwell thermal equilibrium [25]. Thus, I made numerical tests with the Metropolis algorithm for the Maxwell distribution. The obtained results reproduce the functional dependences found in reference [20] (see Eqs. (4, 5) there) with approximately the same values of

the numerical constants. This gives independent confirmation that the Metropolis algorithm treats correctly a weak external perturbation that drives the system out of equilibrium. It also shows that various thermal distributions can be treated by this method.

The model I described assumes that the electrons are non interacting. To be valid it requires that the Coulomb interaction between electrons in 2DES $E_{ee} \approx e^2 \sqrt{\pi n_e} / \epsilon_r$ is small compared to the kinetic energy given by $E_F = \pi n_e \hbar^2 / m$. Here n_e is the electron density, ϵ_r is the dielectric constant, e is the electron charge and m is the effective electron mass. Thus the effective strength of interaction is characterized by the dimensionless parameter $r_s = E_{ee} / E_F$ [29] which should be small. Its value for experimental 2DES obtained in *GaAs/AlGaAs* heterostructure with electron densities $n_e \approx 10^{12} \text{ cm}^{-2}$, an effective electron mass $m \approx 0.065 m_e$ and dielectric constant $\epsilon_r = 13$ is approximately $r_s \sim 1$. At such values the interaction between quasiparticles is considered to be weak and is usually neglected in a first approximation [21, 29], for example the Wigner crystal typically appears at $r_s \approx 37$.

At such densities n_e inside a cell of size $S = 1 \mu\text{m}^2$ the quantum level number of an electron at the Fermi energy is $N_F = n_e S \sim 10^4$. Therefore electrons are in a deep semiclassical regime and the classical Monte Carlo approach used above is well justified, see also [24].

3 Numerical results

I have investigated the dependence of v_f on several system parameters which are relevant for a realistic experiments with 2DES in antidot lattices. Among them are the temperature T , the microwave field strength f and the microwave frequency ω . The effects of geometry are studied by changing the lattice constant R that allows to choose the optimal regime where the photogalvanic effect is stronger. The effects of impurity scattering is modeled by variation of scattering time τ_i that gives insight on the stability of the effect in respect to experimental imperfections. At last the effect of magnetic field is also analyzed.

The temperature dependence for a typical set of parameters is given in Figure 5. The obtained numerical data show that there is a weak drop of the ratchet velocity v_f with the increase of temperature T . However in the regime with $T \ll E_F$, v_f is practically temperature independent. This dependence is preserved for various radiation strengths f . The velocity of transport increases with the growth of f . A detailed study of the effect dependence on the microwave field f is presented in Figure 6. It shows that the dependence on f is quadratic in the region $T \ll E_F$, and temperature independent in a large interval of field strength. At higher f a deviation from the quadratic dependence starts to be visible, this deviation starts earlier at high temperatures. Thus on the basis of the results presented in Figures 5, 6 it is possible to conclude that at $T \ll E_F$ and in the limit of weak driving

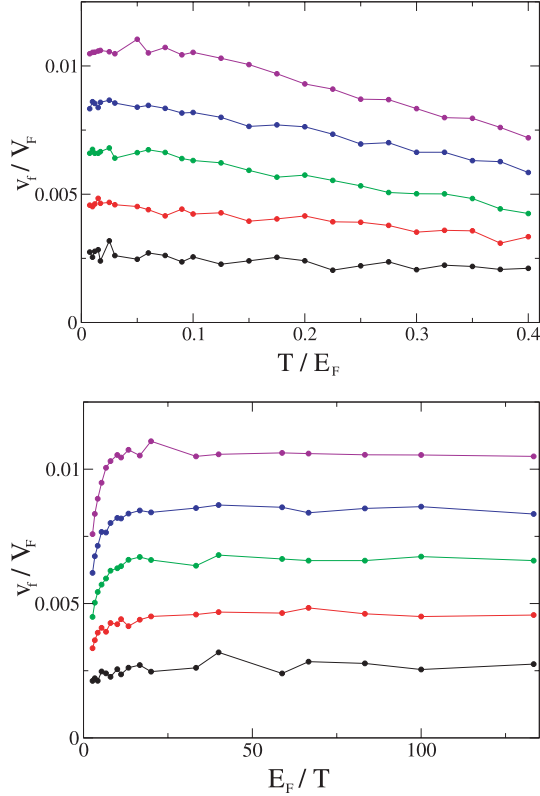


Fig. 5. (Color online) Top panel: dependence of the rescaled flow velocity v_f/V_F on the rescaled temperature T/E_F , different curves correspond to $f = 7.0, 6.0, 5.0, 4.0, 3.0$ (from top to bottom). Bottom panel: the same data are shown as a function of E_F/T . Here $\omega = 1$, $R = 2$, $\theta = 0$.

the flow velocity is described by the relation:

$$v_f/V_F = C(r_d f/E_F)^2. \quad (1)$$

Here the dimensionless factor C may depend on the microwave frequency, lattice geometry, and impurity scattering time. However it is independent of T and f . For $R = 2$, $\omega r_d/V_F \ll 1$ and $\tau_i V_F/r_d \gg 1$ the obtained data give $C = 0.129 \pm 0.002$.

The dependence (1) is qualitatively different from the theoretical estimates proposed in reference [20]. To understand the origin of this difference I remind the main elements of estimates given in references [19,20]. They are based on the fact that the microwave radiation produces diffusive energy growth of electron energy in time with the rate: $D_E = (\delta E)^2/\delta t$. Here δE is the energy variation after a time δt . In the limit of low frequency driving it is possible to write $D_E \sim (\dot{E})^2 \tau_c \sim f^2 V_F l$ where E is the particle energy and l is the mean free path which is $l \sim R^2/r_d$. If a particle would experience a friction force $\mathbf{f}_f = -m\gamma\mathbf{v}$, the diffusion in energy would give energy variation $(\delta E)^2 \sim D_E/\gamma$. In reference [20] it was assumed that δE is fixed by the thermal distribution so that $\delta E \sim T$. Thus the statistical stationary distribution imposes an effective friction with coefficient $\gamma \sim D_E/T^2$. This relation is important because the ratchet velocity is given by relation $v_f \sim l\gamma$ in the limit

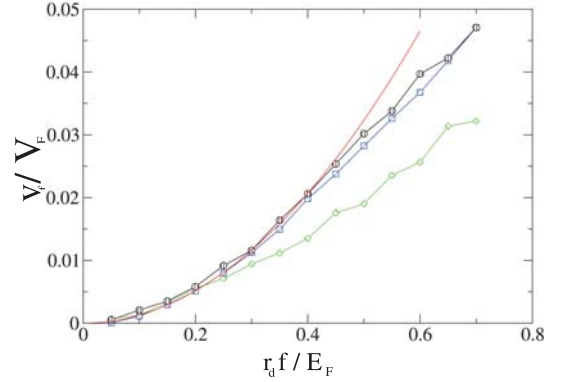


Fig. 6. The rescaled flow velocity v_f/V_F as a function of rescaled applied force $r_d f/E_F$ for different temperatures: $T/E_F = 0.4$ (green diamonds), 0.1 (blue squares), 0.01 (black circles). The red (full gray) curve shows a parabolic fit of data $v_f/V_F = C (r_d f/E_F)^2$ with $C = 0.129 \pm 0.002$ at $T/E_F = 0.01$ (the fit is done in the interval $[0, 0.45]$). Here $\omega = 1$, $R = 2$, $\theta = 0$.

of weak friction as it has been shown in reference [19] by extensive numerical simulations. For the Maxwell distribution this gives $v_f \sim (lf)^2/T^{3/2}m^{1/2}$ since in this case $D_E \sim f^2(T/m)^{1/2}l$, where it is used that the thermal velocity $v \sim \sqrt{T/m}$. The extension of the above arguments to the Fermi-Dirac distribution led the authors of [20] to the conclusion that $v_f/V_F \sim C(fl/T)^2$. However this expression is drastically different from equation (1) according to which there is no temperature dependence in the limit $T \ll E_F$. This contradiction can be resolved if the variation of particle energy induced by the radiation is of the order $\delta E \sim E_F$ (and not $\delta E \sim T$). Indeed in the free electron model the particle can move in the whole energy interval defined by the Fermi energy whereas in the estimates in reference [20] it was assumed that the particle can move only in the narrow thermal layer near the Fermi surface. In the free particle model it is therefore rather natural that the particle energy variation is $\delta E \sim E_F$, that leads to the result of equation (1).

The fact that the free electron model remains valid in the presence of microwave driving can be also understood from the following arguments. For non interacting electrons the Hamiltonian is given by the sum of one particle operators (microwave driving is also one particle operator). Hence, the many particle state (wave function or density matrix) is obtained simply from one particle states by antisymmetrization. Thus, the Pauli principle can be taken into account by averaging the final one particle results over the Fermi-Dirac distribution. This statement also explains the validity of the classical kinetic Boltzmann equation for the description of transport properties of metals. It is demonstrated more rigorously in (Chap. 5 in Refs. [21] and [30]). As a result the limit of weak interactions the Pauli principle does not affect the semiclassical dynamics of the electrons and the arguments presented in reference [20] are not valid at least for weak r_s values.

It is important to stress that the same question has been considered in microscopic models of heavy ions

collisions [31], in laser ionization of metallic clusters [32] and in solid state physics [26,27]. It has been shown (see e.g. [31]) that in the quantum case the distribution function $f_V(\mathbf{r}, \mathbf{p}, t)$ of the fermions obeys the Vlasov-Ühling-Uhlenbeck equation that reads:

$$\frac{\partial f_V}{\partial t} + \mathbf{v} \frac{\partial f_V}{\partial \mathbf{r}} + \mathbf{F}(\mathbf{r}, t) \frac{\partial f_V}{\partial \mathbf{p}} = I_{cc} \quad (2)$$

where $\mathbf{F}(\mathbf{r}, t)$ is an external time dependent Hamiltonian force like a microwave driving and I_{cc} is the collision integral that takes into account electron-electron interactions and other inelastic effects. It explicitly takes into account the Pauli blockade by the mean of $(1 - f_V)$ factors. It should be stressed that the effects of microwave driving are taken into account in the left side of the equation where Pauli blockade is absent which is reflected by the absence of the $(1 - f_V)$ factors. In the case of weak inelastic scattering and weakly interacting electrons, as considered here (in fact non interacting 2DES is treated in this model), the collision integral can be written in the τ approximation [26] as $I_{cc} = -(f_V - f_0)/\tau$ where f_0 is the Fermi-Dirac distribution and τ gives the relaxation time to equilibrium. This expression becomes exact in the limit of weak interaction and high quantum numbers. This corresponds exactly to the situation analyzed here where electron-electron interaction is weak ($r_s < 1$) and the quantum numbers of electrons in one cell are very high $N_F \sim 10^4$. In this case the Fermi-Dirac statistics appears only through the equilibrium distribution f_0 and Pauli blockade does not affect the dynamics. This fact has been analyzed in great detail in [31,32]. The Metropolis algorithm effectively simulates equation (2), indeed the left side is taken into account exactly via the dynamical equations of motion while the Metropolis steps ensure an exponential decay to the equilibrium distribution f_0 as in the τ approximation.

The estimates based on the interplay between diffusive energy excitation and dissipation allow to understand the physical origin of the relation between the ratchet velocity and effective friction coefficient induced by microwave radiation that perturbs the system out of thermal equilibrium. Another approach has been developed recently in reference [33] using perturbation theory for the Boltzmann kinetic equation in the limit of weak radiation and weak density of randomly distributed asymmetric scatterers, the kinetic equation is written in the τ approximation and has the form of equation (2). The model proposed in reference [33] is rather different from the one considered here, e.g. scatterers are distributed randomly on the plane, their density is required to be small and impurity scattering is necessary for the regularization of the model. However in spite of these differences the global dependence of ratchet velocity on Fermi energy E_F and radiation strength f is the same as in equation (1). In particular the temperature dependence is absent for $T \ll E_F$ that corresponds to the absence of Pauli blockade and to the numerical results obtained here.

The frequency dependence of v_f/V_F is shown in Figure 7. The data presented there demonstrate that the

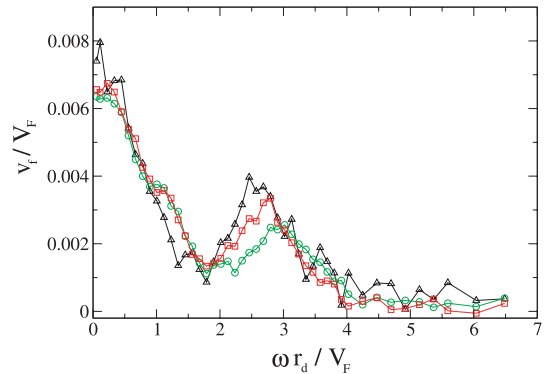


Fig. 7. (Color online) Dependence of rescaled flow velocity v_f/V_F on the rescaled microwave frequency $\omega r_d/V_F$, for $T/E_F = 0.01$, $f = 5.0$ (red squares); $T/E_F = 0.1$, $f = 5.0$ (green circles); and $T/E_F = 0.01$, $f = 3.0$ (black triangles, in this case v_f is multiplied by factor $(5/3)^2$ to underline quadratic dependence on f). Here $R = 2$, $\theta = 0$.

frequency spectrum is independent of temperature (for $T \ll E_F$) and that quadratic dependence on f is valid for a large frequency range. The spectral dependence has a few characteristic features. For $\omega r_d/V_F \ll 1$ the ratchet velocity becomes independent of ω , that is in agreement with the fact that $D_E \propto v_f$ is independent of ω . This has been also seen in models analyzed in references [19,20]. For $\omega r_d/V_F \gg 1$ the ratchet velocity drops with ω . This is consistent with the dependence of D_E on ω which in this limit can be estimated as $D_E \sim f^2 V_F^3 / \omega^2 l$. This comes from the fact that at high frequency the change of velocity after one collision with semidisks is $\Delta v \sim f/\omega m$ so that the energy is changed by $\delta E \sim V_F f/\omega$ after a time between two collisions $\delta t \sim l/V_F$ ($l \sim r_d$ for $R \sim r_d$ and $l \sim R^2/r_d$ for $R \gg r_d$). The frequency dependence shown in Figure 7 has also a resonance at $\omega r_d/V_F \approx 3$. This is probably related to high frequency collisions in narrow bottle necks between two semidisks (see Fig. 1 where the narrow bottle neck is approximately by a factor of three smaller than disk radius).

The dependence of v_f on the distance between disk centers R is shown in Figure 8. Initially v_f starts to grow with R then reaches a maximum value and drops at large R values. The position of the maximum depends on the microwave frequency. With the increase of frequency the maximum moves to smaller values of R . Qualitatively this corresponds to the situation when the microwave frequency becomes comparable with the frequency of collisions of particles with semidisks. The dependence of data on parameters can be satisfactorily described by a fit formula:

$$v_f/V_F = A \frac{R^2 f^2}{E_F^2} \frac{1}{1 + B(\omega R^2/r_d V_F)^2}. \quad (3)$$

Here A, B are dimensionless fitting parameters. The fit for three values of ω in Figure 8 gives $A \approx 0.017$ and $B \approx 0.012$. For $\omega \rightarrow 0$ this expression is in a satisfactory agreement with the value $C \approx 0.13$ found in Figure 6 at $R = 2$. The physical origin of this fit is related to frequency dependence of the diffusion rate D_E which interpolates

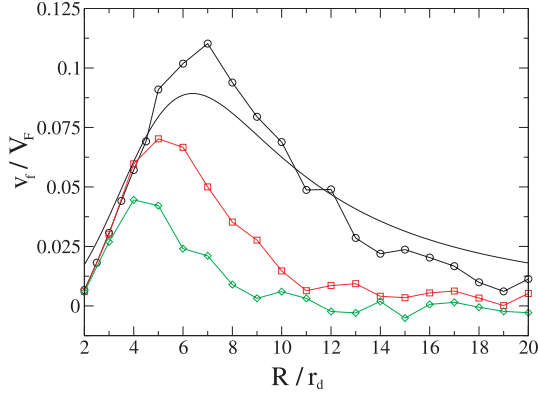


Fig. 8. Dependence of v_f/V_F on the rescaled distance between semidisk centers R/r_d for different frequency values $\omega = 1, 1.5, 2.0$ (curves from top to bottom). The smooth curve shows the fit of equation (2) for $\omega = 1$ with $A = 0.017$, $B = 0.012$. Here $f = 5.0$, $\omega = 1$, $\theta = 0$, $T/E_F = 0.1$.

between the low frequency regime (D_E independent of ω) and the high frequency regime where D_E drops quadratically with ω (see estimates given above). Equation (2) gives reasonable description of obtained numerical data in the regime where l is not too large compared to R . This situation is most interesting for direct experimental studies where R is not very large compared to r_d .

Another important experimental parameter is the scattering time induced by impurities which are always present in real samples. The data presented in previous figures were obtained in the regime of very large τ_i . The effect of finite values of τ_i on the ratchet velocity is described in Figure 9 for various lattice constants R . The data show that at large τ_i values v_f is independent of the impurity scattering time while at small τ_i , v_f/V_F drops approximately linearly with $\tau_i V_F/r_d$. Indeed the asymmetry of semidisks is washed out by impurity scattering and the ratchet effect should disappear at small τ_i . At the same time it is important to stress that the presence of impurities is not necessary for the onset of directed transport. In experimental conditions τ_i can depend on temperature because of electron-phonon scattering or electron-electron interactions which give a dependence of τ_i on T . This may lead to a significant temperature dependence of the photogalvanic effect at higher temperatures where the electron-phonon scattering starts to play a major role.

Experimentally it is also possible to study the dependence of the effect on magnetic field B perpendicular to the 2DES plane. To investigate this dependence the method described above was adapted to the presence of a magnetic field, which was included in the analytical solution of motion equations between Metropolis thermalization steps. The magnetic field dependence is given in Figure 10. The data clearly shows that the ratchet effect disappears for sufficiently strong magnetic fields when the Larmor radius $r_l = V_F/B$ becomes smaller than the distance R between semidisks (here electron charge and mass are set to 1). Indeed for $r_l \ll R$ the classical electron dynamics becomes integrable and the diffusion rate in energy

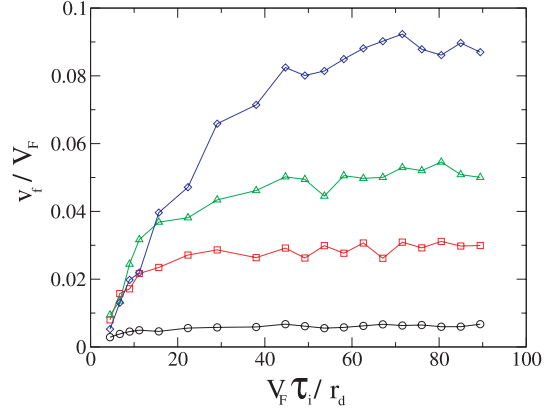


Fig. 9. (Color online) Dependence of v_f/V_F on the rescaled impurity scattering time $V_F \tau_i/r_d$ for $R/r_d = 6.0, 4.0, 3.0, 2.0$ (from top to bottom respectively at $V_F \tau_i/r_d = 50$). Here $f = 5.0$, $\omega = 1$, $\theta = 0$, $T/E_F = 0.1$.

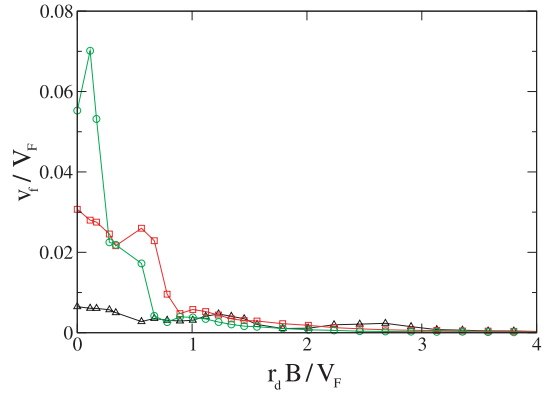


Fig. 10. (Color online) Dependence of v_f/V_F on the rescaled magnetic field $r_d B/V_F$ for $R/r_d = 4.0, 3.0, 2.0$ (curves from top to bottom at $r_d B/V_F = 0$). Here $f = 5.0$, $\omega = 1$, $\theta = 0$, $T/E_F = 0.1$.

D_E goes to zero due to absence of chaos, thus leading to the disappearance of ratchet ($v_f \propto D_E$). In principle the magnetic field changes the transport direction (angle ψ). I do not discuss this dependence here since the main point is that the ratchet effect disappears at relatively low B (see below).

4 Conclusions

The obtained results clearly shows the existence of zero mean force ratchet in asymmetric semiconductor structures induced by microwave radiation. They give the following dependence for the strength of the stationary current induced by the ratchet effect in one row of semidisks (row width $\sqrt{3}R$):

$$I = \sqrt{3}en_e R v_f = A \sqrt{\frac{6}{\pi^2}} \frac{f^2}{n_e^{1/2}} \frac{emR^3}{\hbar^3} \quad (4)$$

where $E_F = \pi n_e \hbar^2/m$ and $m = 0.065m_e$. This dependence holds in the low frequency regime which is usually satisfied at typical electron densities $n_e = 10^{12} \text{ cm}^{-2}$

where the collision frequency is of the order of 200 GHz for a $R \sim 1 \mu\text{m}$ and under the assumption $R \sim r_d$. For $R = 1 \mu\text{m}$ and $f/e = 1 \text{ V/cm}$, equation (3) gives the current 0.1 nA. In samples with high mobility the mean free path can have values as high as $5 \mu\text{m}$, and therefore the optimal regime for photogalvanic effect will be when R is of the same order and it is quite possible that in this situation the current per row can be as high as 10 nA. According to the results of Figure 10 for $R \sim 1 \mu\text{m}$ the ratchet effect starts to disappear at magnetic field $B \sim 0.1 \text{ T}$.

The asymmetric antidot lattice can be considered as a prototype for transport in asymmetric molecular structures. The latter have attracted recently a significant interest in view of possible biological applications of ratchets [34]. Therefore experimental investigations on the ratchet effect discussed in this paper are highly desirable.

I thank D.L. Shepelyansky for stimulating discussions and for his interest in this research. I am also grateful to M.V. Entin, and L.I. Magarill for access to their unpublished results on their kinetic equation approach to the photogalvanic effect. This research is done in the frame of the ANR PNANO project MICONANO.

References

1. E.M. Baskin, L.I. Magarill, M.V. Entin, Sov. Phys.-Solid State **20**, 1403 (1978) [Fiz. Tver. Tela **20**, 2432 (1978)]
2. V.I. Belinicher, B.I. Sturman, Sov. Phys. Usp. **23**, 199 (1980) [Usp. Fiz. Nauk **130**, 415 (1980)]
3. R.D. Astumian, P. Hänggi, Physics Today **55** (11), 33 (2002)
4. P. Reimann, Phys. Rep. **361**, 57 (2002)
5. J.B. Majer, J. Peguiron, M. Grifoni, M. Tussveld, J.E. Mooij, Phys. Rev. Lett. **90**, 056802 (2003)
6. J.E. Villegas, S. Savel'ev, F. Nori, E.M. Gonzalez, J.V. Anguita, R. Garcia, J.L. Vicent, Science **302**, 1188 (2003)
7. A.V. Ustinov, C. Coqui, A. Kemp, Y. Zolotaryuk, M. Salerno, Phys. Rev. Lett. **93**, 087001 (2004)
8. C. Mennerat-Robilliard, D. Lucas, S. Guibal, J. Tabosa, C. Jurczak, J.-Y. Courtois, G. Grynberg, Phys. Rev. Lett. **82**, 851 (1999)
9. S. Matthias, F. Müller, Nature **424**, 53 (2003)
10. V. Studer, A. Pepin, Y. Chen., A. Ajdari, Analyst **129**, 944 (2004)
11. D. Weiss, M.L. Roukes, A. Menschig, P. Grambow, K. von Klitzing, G. Weimann, Phys. Rev. Lett. **66**, 2790 (1991)
12. G.M. Gusev, Z.D. Kvon, V.M. Kudryashov, L.V. Litvin, Y.V. Nastaushv, V.T. Dolgoplov, A.A. Shashkin, JETP Lett. **54**, 364 (1991) [Pis'ma Zh. Eksp. Teor. Fiz. **54**, 369 (1991)]
13. F. Galton, *Natural inheritance* (Macmillan, London, 1889)
14. I.P. Kornfeld, S.V. Fomin, Ya.G. Sinai, *Ergodic theory* (Springer, Berlin, 1982)
15. R. Fleischmann, T. Geisel, R. Ketzmerick, Phys. Rev. Lett. **68**, 1367 (1992); Europhys. Lett. **25**, 219 (1994)
16. A.A. Bykov, G.M. Gusev, Z.D. Kvon, V.M. Kudryashov, V.G. Plyukhin, Pis'ma Zh. Eksp. Teor. Fiz. **53**, 407 (1991) [JETP Lett. **53**, 427 (1991)]
17. H. Linke, T.E. Humphrey, A. Löfgren, A.O. Sushkov, R. Newbury, R.P. Taylor, P. Omling, Science **286**, 2314 (1999)
18. In reference [17] the frequency of AC driving is 191 Hz; this is much smaller than all relaxation rates and smaller than the energy spacing between adjacent quantum levels inside one cell $\Delta/\hbar \sim 1 \text{ GHz}$; therefore the regime discussed in this paper doesn't work for so low frequencies as discussed in [20]
19. A.D. Chepelianskii, D.L. Shepelyansky, Phys. Rev. B **71**, 052508 (2005)
20. G. Cristadoro, D.L. Shepelyansky, Phys. Rev. E **71**, 036111 (2005)
21. J. Rammer, *Quantum Transport Theory* (Perseus books, Reading Massachusetts, 1998)
22. W.G. Hoover, *Time Reversibility, Computer Simulation and Chaos* (World Scientific, Singapore, 1999)
23. Private communication of authors of reference [20] (2005)
24. C. Jacoboni, P. Lugli, *The Monte Carlo method for semiconductor device simulation* (Springer, Wien, 1989)
25. N. Metropolis, A.W. Rosenbluth, M.N. Rosenbluth, A.H. Teller, J. Chem. Phys. **21**, 1087 (1953)
26. N.W. Ashcroft, N.D. Mermin, *Solid state physics* (Holt, Rinehart and Winston New York, 1976)
27. A.A. Abrikosov, *Fundamentals of the theory of metals* (Elsevier Science, Amsterdam, 1988)
28. E. Akkermans, G. Montambaux, *Physique mésoscopique des électrons et des photons* (EDP Sciences, Les Ulis, 2004)
29. E. Abrahams, S.V. Kravchenko, M.P. Sarachik, Rev. Mod. Phys. **73**, 251 (2001)
30. B.I. Sturman, Uspkhi Fiz. Nauk **144**, 497 (1984)
31. G.F. Bertsch, S. Das. Gupta, Phys. Rep. **160**, 189 (1988)
32. F. Calvayrac, P.-G. Reinhard, E. Suraud, C.A. Ullrich, Phys. Rep. **337**, 493 (2000)
33. M.V. Entin, L.I. Magarill, private communication July 2005; e-print [arXiv:cond-mat/0512437](https://arxiv.org/abs/cond-mat/0512437)
34. F. Jüllicher, A. Ajdari, J. Prost, Rev. Mod. Phys. **69**, 1269 (1997)